



HOKKAIDO UNIVERSITY

Title	Conductance Gap Anomaly in Scanning Tunneling Spectra of MBE-Grown (001) Surfaces of III-V Compound Semiconductors
Author(s)	Kasai, Seiya; Neguro, Noboru; Hasegawa, Hideki
Citation	Applied Surface Science, 175-176, 255-259 https://doi.org/10.1016/S0169-4332(01)00093-9
Issue Date	2001-05-15
Doc URL	https://hdl.handle.net/2115/8365
Type	journal article
File Information	ICSFS.pdf



Conductance Gap Anomaly in Scanning Tunneling Spectra of MBE-Grown (001) Surfaces of III-V Compound Semiconductors

Seiya KASAI, Noboru NEGORO and Hideki HASEGAWA

Research Center for Interface Quantum Electronics and

Graduate School of Electronics and Information Engineering, Hokkaido University

North 13, West 8, Kitaku, Sapporo, 060-8628, Japan e-mail: kasai@rciqe.hokudai.ac.jp

Abstract

A scanning-tunneling-spectroscopy (STS) study was performed on MBE-grown (001) surfaces of GaAs, Al_{0.3}Ga_{0.7}As and In_{0.53}Ga_{0.47}As in an ultrahigh vacuum (UHV) STS system to clarify microscopic behavior of surface states causing Fermi level pinning on these III-V compound semiconductor surfaces. On all the sample surfaces, there existed spots which showed anomalous STS spectra showing conductance gaps much larger than the energy gap of the material. The rates of finding such spots as well as the magnitudes of the anomalous conductance gap were strongly material-dependent, increasing in the order of InGaAs, GaAs and AlGaAs. Scanning tunneling microscope (STM) images under low-positive sample biases showed dark areas which gradually decreased with the increase of the positive sample bias, and correlated with the spatial variation of conductance gaps of the STS spectra. On the basis of a detailed computer simulation, the conductance gap anomaly is explained by a tip-induced local charging of surface states where the apparent gap width depends on surface state distribution shape and density. The result shows that an extremely high density of surface states exist on the AlGaAs surface, but not so much on the InGaAs surface with the GaAs surface in between.

Keywords: Scanning tunneling spectroscopy; conductance gap; GaAs; InGaAs; AlGaAs; surface state

1. Introduction

The recent remarkable progress of nano-fabrication technology of III-V compound semiconductors has realized not only high-speed and low-power operations of conventional electronic and optoelectronic devices but also opened up a future possibility of various quantum devices. This trend, on the other hand, has increased the importance of surfaces and interfaces a great deal, since they are more and more strongly related to the device performance with the reduction of feature sizes. In order to obtain well-behaved III-V devices in nano-scale, it is important to understand and control, in atomic scale, the behavior of surface states that cause well-known Fermi level pinning phenomena.

Scanning tunneling spectroscopy (STS) seems to be powerful tool for such a study. However, only limited work has been done so far on technologically important (001) III-V compound semiconductor surfaces[1-5] as compared with many studies on vacuum cleaved (110) surfaces initiating from the work by Feenstra *et al.*[6-8]. STS spectra on (001) GaAs surfaces showed anomalously large conductance gaps, but did not show surface states in the conductance gap regions as indicated by Feenstra *et al.*[7,8]. To explain this, we proposed a novel model based on a tip-induced local surface state charging and pointed out the correlation between the surface state density and the rate of finding anomalous spectra[4,5].

In this paper, spectroscopic properties of surface states on MBE-grown (001) surfaces of GaAs, $\text{Al}_{0.3}\text{Ga}_{0.7}\text{As}$ and $\text{In}_{0.53}\text{Ga}_{0.47}\text{As}$ are studied by an STS installed in an ultrahigh vacuum (UHV)-based multi-chamber growth/characterization system. The novel proposed model[4,5] was further extended and applied to the explanation of the experimental results. Topological features on scanning tunneling microscope (STM) images were also correlated with spatial distributions of STS conductance gaps.

2. Experimental

The experiments were done in an UHV-based multi-chamber system having MBE,

UHV STM/STS, X-ray photoelectron spectroscopy (XPS), and contactless capacitance-voltage (C-V) and other chambers. Firstly, Si-doped (001) GaAs, Al_{0.3}Ga_{0.7}As lattice-matched to GaAs and In_{0.53}Ga_{0.47}As lattice-matched to InP were grown on n⁺-GaAs and n⁺-InP substrates, respectively, by a conventional solid-source MBE. Si doping concentration was $2-5 \times 10^{18} \text{ cm}^{-3}$. Then, the samples were transferred into the UHV STM/STS chamber and measurements were done without breaking the UHV condition. STM images and STS spectra were taken using JEOL JSTM-4600 microscope. Surface Fermi level positions and surface state distribution were also characterized macroscopically by XPS and contactless C-V techniques and they were compared with STS results.

3. Experimental results

Figure 1(a), (b) and (c) show typical STS spectra obtained on MBE-grown (001) GaAs, Al_{0.3}Ga_{0.7}As and In_{0.53}Ga_{0.47}As surface, respectively. Normal STS spectra having conductance gaps which equal to the band gap of the material were obtained only on limited spots on the GaAs and InGaAs surfaces, but no at all on the AlGaAs surface. On the other hand, anomalous spectra showing conductance gaps much larger than the band gap were seen on all the sample surfaces. Typical conductance gap widths were 2 ~ 3 V. Surface Fermi level positions (E_{FS}) evaluated from the normal spectra for GaAs and InGaAs surface were 0.83 eV and 0.36 eV from conduction band edge (E_C), respectively, and these values were consistent with macroscopically obtained positions of E_{FS} by XPS and contactless C-V measurements.

A large number of STS spectra were taken on the wide area of sample surfaces, and the number of spots of showing normal and anomalous spectra were counted. The rates of detecting anomalous STS spectra were 81 % for GaAs, 61 % for InGaAs and 100 % for AlGaAs. It was also found that the width of the conductance gap on the anomalous STS spectra varied from one spot to another even on the same sample surface.

In order further to correlate spatial distributions of conductance gaps with the STM

images, bias-dependent STM images were taken. As an example, Figure 2 shows bias-dependent STM images taken on the (2x4) GaAs (001) surface. By such measurements, it was found that the light regions in STM images corresponded to the spots with small conductance gaps in the STS spectra and that the areas keeping dark images over a wide sample bias range corresponded to spots with large conductance gaps in the STS spectra. In both cases of high negative and positive sample biases, clear atomic-scale images could be obtained as seen in Fig.2. However, as the positive sample bias (empty state bias) was reduced, the images started to show inhomogeneous dark areas, and such areas gradually increased. The image almost vanished when sample bias, $V_S = +2.2$ V. A similar trend was also seen under negative bias (filled state bias), but to a much lesser extent. These features showed strong correlation with the spatial distribution of the width of the conductance gap on the sample surface. However, no direct one-to-one correlation between the any of specific structural defect in atomic scale on the surface and the dark area in the STM image could be found.

4. Discussion

The conductance gap anomaly in STS spectra was reported previously on GaAs (001) surfaces[1,3-5]. In this study, it was found that this anomaly also takes place on AlGaAs and InGaAs surfaces. On the other hand, Pashley *et al.*[2] performed STS measurements on GaAs(001) surfaces, and their STS spectra showed the normal GaAs energy gap. This anomaly does not seem to be explicable in terms of the previously proposed model paying attention to the spreading resistance effect[9], since the carrier concentration was sufficiently high in these experiments. An attempt to explain the anomaly in terms of change of the surface band bending electrostatically induced by the STM tip was made by Bressler-Hill *et al.*[1]. They assumed that surface band bending was caused by discrete deep acceptor surface states near midgap whose occupancy was determined by the semiconductor bulk Fermi level, and they treated the problem using the one-dimensional (1D) theory for a macroscopic

metal-insulator-semiconductor (MIS) structure. However, in the conventional STS measurement system, the tip is so sharp and validity of such 1D treatment is recently questionable.

As an alternative model, we have proposed recently a new model based on where highly localized charging of the surface states due to direct supply or removal of electrons by the STM tip changes locally the magnitude of the surface band bending, and causes the observed anomaly[4,5]. Here, we assumed that the occupancy of the surface states is dynamically determined by the tip Fermi level rather the semiconductor bulk Fermi level due to fast tunneling into surface states and slow thermal escape of electrons from surface states.

In this study, we attempted quantitative confirmation of such a situation. According to our idea, the STM tip writes charges into the surface states with tunneling rate, T , and the charge emission to the bulk semiconductor also takes place with an emission rate, e_n . In the case of $T \gg e_n$, the surface states are filled and charged with the surface Fermi level being in a dynamic equilibrium with the tip Fermi level, $E_F(\text{tip})$. It should be noted that the principle of the surface state measurements by STS tacitly assumes that states are empty so that the tunneling current becomes proportional to the density of surface states. Figure 3 shows calculated T and e_n as a function of tip-sample distance, d , for various energy depths of surface states assuming a typical surface state capture cross-section value of 10^{-16} cm^2 . It was found $T \gg e_n$ in the case of $d < 1.5 \text{ nm}$. In our measurement, typically $d \sim 1 \text{ nm}$, thus the E_{FS} equals to $E_F(\text{tip})$ and thus surface state charging should take place.

To confirm the quantitative capability of our model in explaining the anomaly, we carried out a three-dimensional (3D) potential simulation, rigorously taking account of the tip shape. From the 3D simulation, it became apparent that electrostatic change of the band bending by the tip as assumed by Bressler-Hill *et al.*[1] was negligible due to extreme small tip capacitance in 3D STM configuration. Figure 4 shows the relative tip potential on GaAs surface vs. sample bias for surface state distributions having various shapes, i.e. discrete acceptor states, discrete donor states, a uniform and continuous distribution of acceptor and donor state with a charge neutrality level E_{HO} and a U-shaped continuous distributions of

donor and acceptor states. All the calculation showed that the usual assumption of the sample bias being totally applied between surface and tip fails due to charging of surface states. Namely, by assuming presence of discrete donor states on the surface, downward movement of the tip potential was hindered at the discrete state level. This results in the extending of the conductance gap in the negative sample bias region. On the other hand, by assuming discrete acceptor states, the upward movement of the tip potential was hindered in the positive sample bias region. The uniform and U-shaped continuous surface state distributions containing both acceptor- and donor-type states hinders the tip potential movement, and causes enlargement of the conductance gap in both positive and negative bias directions, as observed in the experiments.

Figure 5 shows the theoretically calculated conductance gap vs. surface state density, N_{SS} for uniform distribution for GaAs. The width of the conductance were evaluated from the difference between the sample biases at which the tip potential reaches the conduction or valence band edge, respectively. As seen in Fig. 5, the effective gap width increased as the increase of N_{SS} . The conductance gap width of 2 ~ 3 eV seen in the experimental results are thus caused by N_{SS} of $10^{13} \sim 10^{14} \text{ cm}^{-2} \text{ eV}^{-1}$. The variation in STS conductance gap width in the experimental results is explained by the spatial variation of surface states density. The gradual change of the dark areas in the bias-dependent STM images shown in Fig.2 indicates the spatially continuous distribution of surface states rather than localized single discrete surface states, even in the microscopic regime. The wide conductance gap in the AlGaAs STS spectra can be explained by the existence of high density of surface states over $10^{13} \text{ cm}^{-2} \text{ eV}^{-1}$. On the other hand, conductance gaps are only slightly larger than the band gap in the InGaAs STS spectra and this indicates a much lower surface state density. These are consistent with the observed material tendency of the rate of detecting anomalous STS spectra. Finally, the reason why Pashley *et al.*[2] did not see anomalous conductance gap on (001) GaAs with strong Fermi level pinning is probably due to the fact that they used extremely small tunneling current using a special set-up so that electrons escaped from states before causing local charging of states.

5. Conclusion

A scanning-tunneling-spectroscopy (STS) study focusing on the conductance gap anomaly was done on MBE-grown (001) surfaces of GaAs, AlGaAs and InGaAs by an UHV STS and computer simulations.

All the samples showed anomalous STS spectra and the rate of finding anomalous spots depended strongly on the material. STM images with low-positive sample biases showed appearance of inhomogeneous dark areas and they correlated well with the spatial distribution of the conductance gap of STS spectra.

The conductance gap in anomalous STS spectra can be explained by a tip-induced local charging of surface states. The gap width is found to depend on surface state distribution and density. High density of surface states seem to exist on the AlGaAs surface but not so much on the InGaAs surface with the GaAs surface in between.

Reference

- [1] V. Bressler-Hill, M. Wassermeier, K. Pond, R. Maboudian, G. A. D. Briggs, P. M. Petroff, and W. H. Weinberg, *J. Vac. Sci. Technol. B* 10 (1992) 1881.
- [2] M. D. Pashley, K. W. Haberern and R. M. Feenstra, *J. Vac. Sci. Technol B* 10 (1992) 1874.
- [3] T. Takahashi and M. Yoshita, *Appl. Phys. Lett.* 70 (1997) 2162.
- [4] N. Negoro, H. Fujikura and H. Hasegawa, *Appl. Surf. Sci.* 159/160 (2000) 292.
- [5] H. Hasegawa, N. Negoro, S. Kasai, Y. Ishikawa and H. Fujikura, *J. Vac. Sci. Technol. B*, 18 (2000) 2100.
- [6] R. M. Feenstra and J. A. Stroscio, *J. Vac. Sci. Technol. B* 5 (1987) 923.
- [7] R. M. Feenstra and P. Martensson, *Phys. Rev. Lett.* 61 (1988) 447.
- [8] R. M. Feenstra, *Phys. Rev. Lett.* 63 (1989) 1412.
- [9] F. Flores and N. Garcia, *Phys. Rev. B* 30 (1984) 2289.

Figure captions

Fig.1 STS spectra on (a) n-GaAs, (b) n-Al_{0.3}Ga_{0.7}As and (c) n-In_{0.53}Ga_{0.47}As (001) surfaces.

Fig.2 Bias dependence of STM images on GaAs. (a) Positive and (b) negative sample bias conditions.

Fig.3 Tunneling and emission rate of the metal-air gap-GaAs system.

Fig.4 (a) Surface state distributions and (b) STM tip potential vs. sample bias for GaAs.

Fig.5 Effective energy gap width vs. surface state density, N_{SS} .

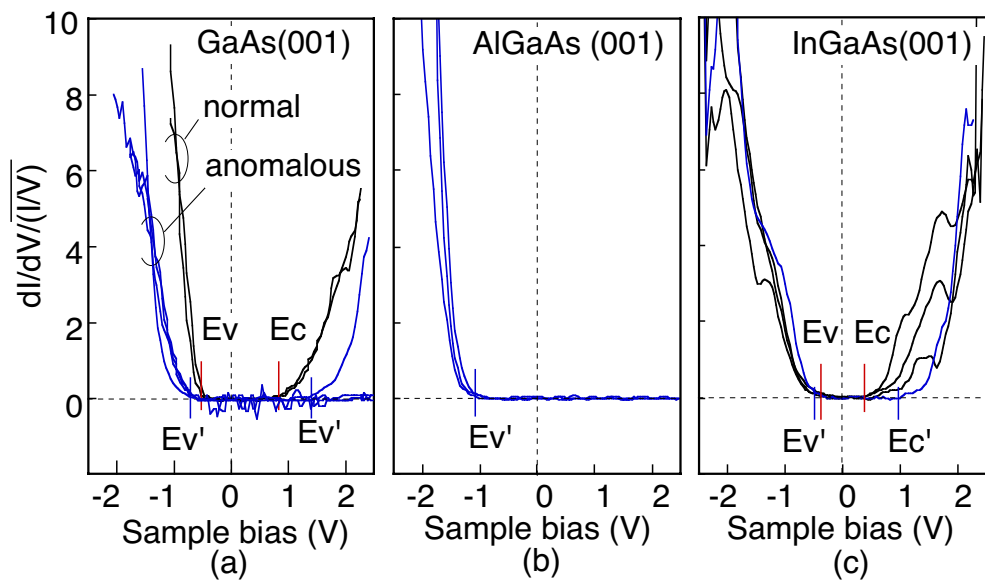
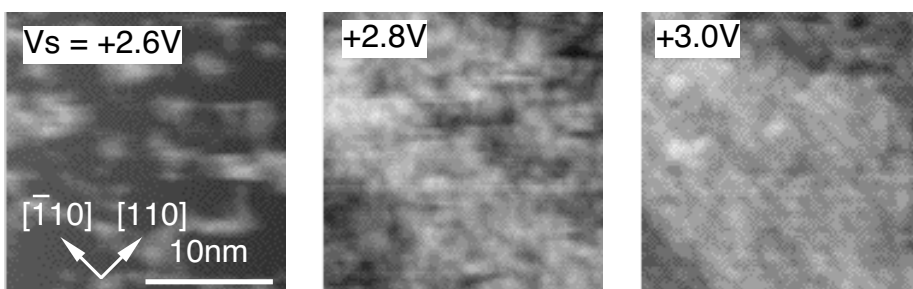
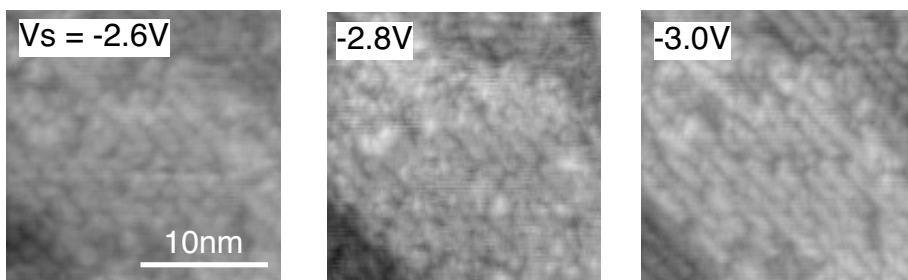


Figure 1, Kasai et al.



(a)



(b)

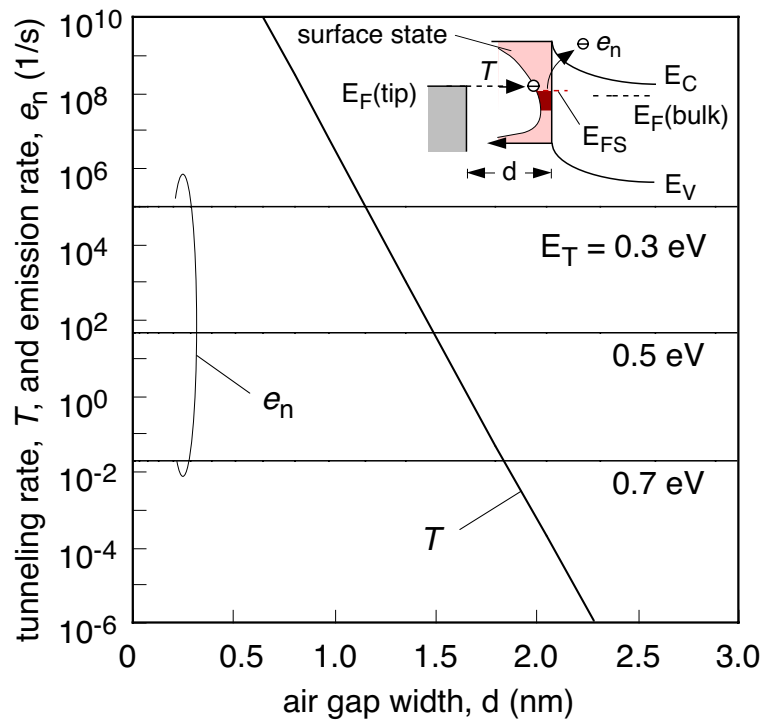
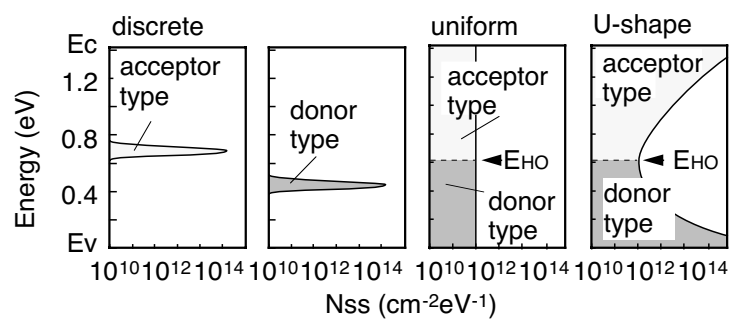
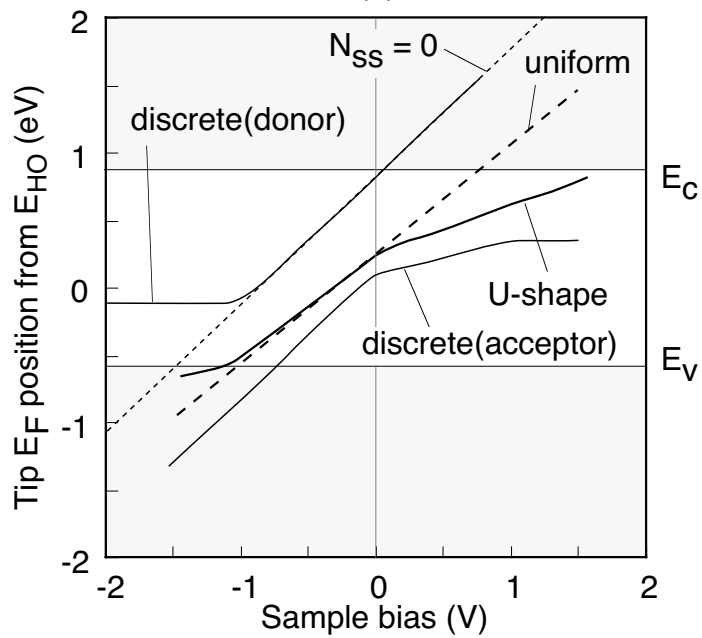


Figure 3, Kasai et al.



(a)



(b)

Figure 4, Kasai et al.

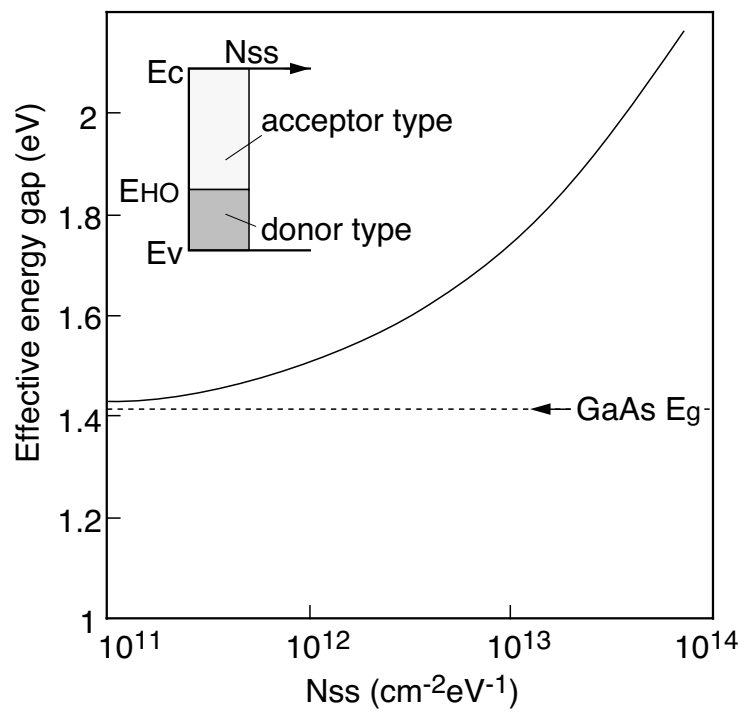


Figure 5, Kasai et al.